Document downloaded from:

http://hdl.handle.net/10251/117217

This paper must be cited as:

Pleguezuelos-Villa, M.; Mir Palomo, S.; Díez-Sales, O.; Vila Busó, MO.; Ruiz-Sauri, A.; Nácher Alonso, MA. (2018). A novel ultradeformable liposomes of Naringin for anti-inflammatory therapy. Colloids and Surfaces B Biointerfaces. 162:265-270. https://doi.org/10.1016/j.colsurfb.2017.11.068

The final publication is available at

http://doi.org/10.1016/j.colsurfb.2017.11.068

Copyright Elsevier

Additional Information

Accepted Manuscript

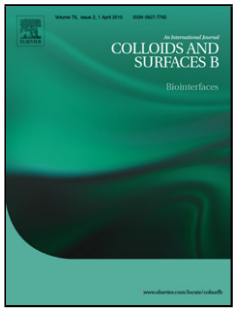

Title: A novel ultradeformable liposomes of Naringin for anti-inflammatory therapy

Authors: María Pleguezuelos-Villa, Silvia Mir-Palomo, Octavio Díez-Sales, M.A. Ofelia Vila Buso, Amparo Ruiz Sauri, Amparo Nácher

PII: S0927-7765(17)30833-0
DOI: https://doi.org/10.1016/j.colsurfb.2017.11.068
Reference: COLSUB 9019

To appear in: *Colloids and Surfaces B: Biointerfaces*

Received date: 28-9-2017
Revised date: 25-11-2017
Accepted date: 30-11-2017

Please cite this article as: María Pleguezuelos-Villa, Silvia Mir-Palomo, Octavio Díez-Sales, M.A.Ofelia Vila Buso, Amparo Ruiz Sauri, Amparo Nácher, A novel ultradeformable liposomes of Naringin for anti-inflammatory therapy, Colloids and Surfaces B: Biointerfaces https://doi.org/10.1016/j.colsurfb.2017.11.068

This is a PDF file of an unedited manuscript that has been accepted for publication. As a service to our customers we are providing this early version of the manuscript. The manuscript will undergo copyediting, typesetting, and review of the resulting proof before it is published in its final form. Please note that during the production process errors may be discovered which could affect the content, and all legal disclaimers that apply to the journal pertain.

ACCEPTED MANUSCRIPT

A novel ultradeformable liposomes of Naringin for anti-inflammatory therapy

María Pleguezuelos-Villa[1, *], Silvia Mir-Palomo[1], Octavio Díez-Sales [1,2], M.A. Ofelia Vila Buso[3], Amparo Ruiz Sauri [4], Amparo Nácher[1, 2].

[1]Department of Pharmacy, Pharmaceutical Technology and Parasitology, Faculty of Pharmacy, University of Valencia, Av. Vicent Andrés Estellés s/n, 46100, Burjassot, Valencia, Spain.

[2]Instituto Interuniversitario de Investigación de Reconocimiento Molecular y Desarrollo Tecnológico (IDM), Universitat Politècnica de València, Universitat de València, Av. Vicent Andrés Estellés s/n, 46100, Burjassot, Valencia, Spain.

[3]Department of Physical Chemistry, Faculty of Pharmacy, University of Valencia, Av. Vicent Andrés Estellés s/n, 46100, Burjassot, Valencia, Spain.

[4] Department of Pathology, University of Valencia, Av. Blasco Ibañez 17, 46010 Valencia, Spain.

***Corresponding author**: M. Pleguezuelos-Villa; e-mail address: maplevi@alumni.uv.es

The article has 4636 words including ackwonledgment and references. The abstract has 127 words. There are 5 figures and 2 tables.

Highlights

- Nanovesicles were small in size and monodispersed independently of the NA concentration.
- No citotoxity effects were observed in 3T3 fibroblasts treated with ultradeformable liposomes.

ACCEPTED MANUSCRIPT

- Ultradeformable liposomes have the ability to reduce skin inflammation.

Graphical abstract

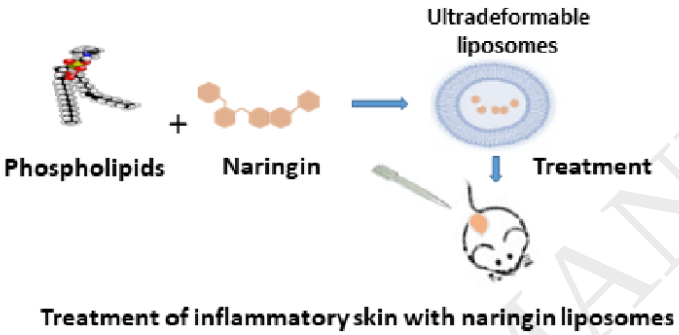

Abstract

Ultradeformable liposomes were formulated using naringin (NA), a flavanone glycoside, at different concentrations (3, 6 and 9 mg/mL). Nanovesicles were small size (~100 nm), regardless of the NA concentration used, and monodisperse (PI < 0.30). All formulations showed a high entrapment efficiency (~88%) and a highly negative zeta potential (around -30 mV). The selected formulations were highly biocompatible as confirmed by *in vitro* studies using 3T3 fibroblasts. *In vitro* assay showed that the amounts (%) of NA accumulated in the epidermis (~ 10%) could explain the anti-inflammatory properties of ultradeformable liposomes. *In vivo* studies confirmed the higher effectiveness of ultradeformable liposomes respect to betamethasone cream and NA dispersion in reducing skin inflammation in mice. Overall, it can conclude that NA ultradeformable liposomes can be considered as a promising formulation for the treatment of skin inflammatory diseases.

ACCEPTED MANUSCRIPT

Keywords: naringin, ultradeformable liposomes, anti-inflammatory, transdermal penetration, fibroblasts, *in vivo* studies

ACCEPTED MANUSCRIPT

1. Introduction

The incidence of skin inflammatory diseases (dermatitis, psoriasis, rash) has increased significantly in the last decades and bioflavonoids such as quercetin, curcumin and baicalin have been widely used for treatment of this injures [1,2,3,4]. Citrus fruits peels represent an important source of phenolic acids and flavonoids, mainly polymethoxyflavones (PMFs), flavanones and glycosylated flavanones [5,6]. Naringin (NA), a bioactive component of citrus species, is a glycosylated flavanone formed by naringenin (flavanone) and the disaccharide neohesperidose (Figure 1). This compound shows a wide variety of pharmacological effects such as antioxidant, blood lipid–lowering and anticarcinogenic activity. Moreover, several studies have highlighted its potential to suppress the production of proinflammatory cytokines and attenuate the

ACCEPTED MANUSCRIPT

inflammatory response [7, 8, 9, 10, 11, 12] and it has been proposed in combination with corticoids to treat skin diseases such as dermatitis [13].

On the other hand, most of conventional therapies failed because of their low capacity to deliver therapeutic drug concentrations to the target tissue. Different approaches have been attempted to overcome this problem by providing "selective" delivery of drugs to the affected area, using various pharmaceutical carriers. In the last years, among the different types of particulate carriers, liposomes have received a great attention [14] and have been used as delivery systems of different bioactive agents. The list of actives incorporated in nanoliposomes is huge, ranging from pharmaceutical to cosmetics and nutraceuticals substances (opiods, curcumin, resveratrol, quercetin, silibinin, glycyrrhizic acid, vitamin C, and others) [15,16,17,18,19,20,21]. In general, these systems are able to enhance the performance of the incorporated bioactive agents by improving their solubility and bioavailability, their *in vitro* and *in vivo* stability, as well as preventing their unwanted interactions with other molecules [22, 23]. Another advantage of nanoliposomes is cell-specific targeting, which is a prerequisite to ensure the adequate drug concentrations required for optimum therapeutic effects in the target site while minimizing adverse effects on healthy cells and tissues. Among them, ultradeformable liposomes have been found to be promising for herbal extracts delivery [6,24]. Since, this type of phospholipid vehicles increases the accumulation on the skin as well as reduces adverse effects. Recent reports showed that ultradeformable nanosized liposomes may be postulated as a novel dermal delivery carrier due to their biocompatibility and high elasticity [25, 26], which is attributed to of the combination of phospholipids and surfactant (such as sodium cholate, deoxycholate, Span, Tween and dipotasium glycyrrhizinate). The surfactant acts as an ´edge activator´ that modify the organization of the lipid bilayers increasing its deformability [27].

The purpose of this study is to develop ultradeformable liposomes. To do this, the vesicles were formulated using different concentrations of naringin (NA) and characterized in terms of zeta potential, mean size, size distribution and vesicles encapsulation efficiency. *In vitro* transdermal

ACCEPTED MANUSCRIPT

penetration was also quantified. Cytotoxicity test was carried out as well to evaluate the biocompatibility of the formulations on 3T3 mouse dermal fibroblast cells. In addition, NA ultradeformable liposomes ability to attenuate skin inflammation induced by phorbol 1, 2-myristate 1, 3-acetate (TPA) in mice was studied.

2. Materials and methods

2.1. Materials

Monosodium phosphate was purchased from Panreac quimica S.A. (Barcelona, Spain). Lipoid® S75, a mixture of soybean lecithin containing lysophosphatidylcholine (3% maximum), phosphatidylcholine (70%), phosphatidylethanolamine (10%), fatty acids (0.5% maximum), triglycerides (3% maximum), and tocopherol (0.1–0.2%) were a gift from Lipoid GmbH (Ludwigshafen, Germany). Polysorbate 80 was purchased from Scharlab S.L. (Barcelona, Spain). Glycerin and ethanol were purchased from Guinama S.L.U. (Valencia, Spain), N-octanol (special grade for measurement of partition coefficients) was purchased from VWR chemicals S.A. S (France), Disodium phosphate were purchased from Scharlab S.L. (Barcelona, Spain). Betamethasone was from IFC Acofarma S.A. (Santander, Spain). Phorbol 1,2-myristate 1,3-acetate and naringin with a molecular formula ($C_{27}H_{32}O_{14}$) and weight (580.54 g/mol) were purchased from Sigma-Aldrich.

2.2. Analytical method

A high-performance liquid chromatograph (HPLC) PerkinElmer® Series 200 equipped with an auto-injector and a photodiode array UV detector was used for NA quantification in experimental samples [28]. The column used was a Teknokroma® Brisa "LC2" C18, 5.0 μm (150 cm x 4.6 mm). The mobile phase consisted of a mixture 50:50 (V/V) of methanol and ultrapure water adjusted at pH 4. The detection wavelength was 280 nm, the injection volume was 20 μL and the

ACCEPTED MANUSCRIPT

flow rate was 1.0 mL/min. Linearity, limit of quantification (LOQ), detection (LOD), precision and accuracy of the analytic method were carried out.

2.3. Physicochemical properties

2.3.1. Crystalline structure

NA structure was analyzed with the X-ray diffractometer KAPPA CCD. The system has a goniometer of four circles and a two-dimensional KAPPA CCD detector with beryllium window of 90 mm diameter maintained at - 60°C.

2.3.2. Solubility

The solubility of the flavonoid at 25°C was determined in different vehicles: water, pH 7.4 buffered solution and polysorbate 80 (1%, w/w) in aqueous medium. Flavonoid was added to saturation in each system during 24 hours under constant agitation (500 rpm). Finally, an aliquot of each sample was filtered (0.22 μm) and quantified.

2.3.3. Partition coefficient determination

Octanol-water partition coefficient (P_{oct}) value was obtained by equilibrating the NA aqueous solution with 1-octanol in a shaker bath at 25ºC overnight [29]. Distribution of NA between the aqueous and the organic phase was estimated by the differences between the NA concentration at the beginning and at the equilibrium step, according to the following equation (Eq.1):

$$P_{oct} = \frac{(Co - Ce)/Vo}{Co/Va} \quad \text{Eq.1}$$

where C_o, is the initial NA aqueous solution concentration, C_e, the solution concentration at equilibrium, V_o, volume of the organic phase (50 mL) and V_a, the volume of aqueous solution (50 mL).

ACCEPTED MANUSCRIPT

2.4. Ultradeformable liposomes

A preformulation studies was carried out in order to select the best formulations able to load increasing amount of NA (from 1 to 24 mg/mL). According to stability data (average particle size <150 nm, polydispersity values < 0.5 and zeta potential value < -25 mV), one formulation was selected with different amount of NA: liposomes I (3 mg/mL), liposomes II (6 mg/mL) and liposomes III (9 mg/mL). NA (3 or 6 or 9 mg/mL), polysorbate 80 (2.5 mg/mL) and Lipoid® S75 (120 mg/mL) were added in a glass vial. These mixtures were hydrated overnight at room temperature (25°C) with a buffer phosphate solution (pH 7.4). The obtained dispersions were sonicated for 4 min using an ultrasonic disintegrator (CY-500, Optic Ivymen system, Barcelona, Spain). Then liposome suspensions were extruded through a 0.20 µm membrane with an Avanti® Mini-Extruder (Avanti Polar Lipids, Alabaster, Alabama) to obtain homogeneous dispersions. NA dispersion (9 mg/mL) in phosphate buffer solution containing polysorbate 80 (1%, w/w) and empty liposomes (without NA) were prepared as control.

2.5. Characterization of liposomes

2.5.1. Transmission electron microscopy

Ultradeformable liposomes morphology was examined through a negative staining technique using a JEM-1010 microscope (Jeol Europe, Croissy-sur-Seine, France), equipped with a digital camera MegaView III at an accelerating voltage of 80 Kv.

2.5.2. Determination of entrapment efficiency (EE %)

1 mL of each sample and dialyzed against buffer (100 mL) for 24 hours, at room temperature using a membrane Spectra/Por, (12–14 kDa MW cut-off; Spectrum Laboratories Inc., DG Breda, The Netherlands). Dialyzed and non-dialyzed ultradeformable liposomes were disrupted with methanol (1:100). The samples were assayed by HPLC as described in section 2.2.

ACCEPTED MANUSCRIPT

EE (%) of liposomes I, II and III was calculated as follows (Eq.2):

$$\text{EE } \% = \left(\frac{\text{actual NA}}{\text{initial NA}}\right) \text{X } 100 \qquad \text{(Eq.2)}$$

where actual NA is the amount of the active in ultradeformable liposomes after dialysis, and initial NA is the amount before dialysis.

2.5.3. Determination of vesicle size, zeta potential and polydispersity index

Average diameter and polydispersity index (PI) of the samples were performed in triplicate by means of Photon Correlation Spectroscopy using a Zetasizer Nano-S® (Malvern Instruments, Worcester-shire, United Kingdom) at 25ºC. Moreover, zeta potential was estimated by electrophoretic light scattering in a thermostated cell in a Zetasizer Nano-S®. The ultradeformable liposomes stability was evaluated over 30 days at ~ 4°C.

2.6. Cell viability studies

3T3 mouse fibroblasts (ATCC, Manassas, VA, USA) were cultured in Dulbecco's modified Eagle's medium (DMEM, Sigma Aldrich, Spain), supplemented with penicillin (100 U/mL), 10% (V/V) fetal bovine serum, and streptomycin (100 mg/mL) (Sigma Aldrich, Spain) in 5% CO_2 incubator at 37 °C to maintain cell growth.

3T3 cells ($2x10^5$ cells/well) were seeded in 96-well plates at passage 14-15. After one day of incubation, 3T3 cells were treated with NA dispersion (9 mg/mL) or empty or NA loaded liposomes I, II and III for 24 hours. In each well 25 µL of formulation were added and filled with 225 µL of cultured medium.

Cell viability was evaluated by MTT [3 (4,5-dimethylthiazolyl-2)-2,5-diphenyltetrazolium bromide] colorimetric assay [30]. After 24 h experiment, 100 µL of MTT was added to each well, and then, after 3 h the formazan crystals formed were dissolved in DMSO (50 µL). The reaction

ACCEPTED MANUSCRIPT

was measured at 570 nm with a spectrophotometer. All experiments were repeated three-fold (n=3).

2.7. *In vitro* diffusion

A diffusion study was performed using Franz diffusion cells (with an effective diffusion area of 0.784 cm^2) and new born pig skin from a local slaughterhouse. The receptor compartment (CR) was filled with buffer phosphate solution (pH 7.4), continuously stirred and thermostated at 32ºC. Epidermal membranes were obtained from heat separation through immersing in water (at 60ºC) for 75 s [31]. On the epidermis surface 800 µL of different formulations assayed were applied. At different time intervals up to 24 hours, receptor solutions were withdrawn and assayed for drug content by HPLC, (section 2.2). At the end of the experiment, 1 mL of phenol red solution (0.05%, w/w) was applied in the donor compartment for checking the integrity of the epidermis [32].

2.8. *In vivo* assay

Female CD-1 mice (5–6 weeks old, 25–35 g) were obtained from Harlan laboratories (Barcelona, Spain) and acclimatized for one week before use. All studies were performed in accordance with European Union regulations for the handling and use of laboratory animals and the protocols were approved by the Institutional Animal Care and Use Committee of the University of Valencia (code 2016/VSC/PEA/00112 type 2).

One day before the experiment the back skin of mice (n=4 per group) was shaved. The first day, TPA dissolved in acetone (3 µg/20 µL) was applied to the shaved dorsal area to induce cutaneous inflammation and ulceration. Negative control mice only received acetone (20 µL). After 3 h, 200

ACCEPTED MANUSCRIPT

µL of empty or NA loaded ultradeformable liposomes (I, II and III), NA dispersion or betamethasone cream (20 mg) were topically applied in the dorsal area. The procedure was repeated on the second and third day. The fourth day, mice were sacrificed by cervical dislocation.

Two biomarkers: oedema formation and myeloperoxidase (MPO) activity were used to evaluate the effect of the formulations [33]. First, dorsal skin area was excised, weighed to assess oedema formation and stored at -80°C. Second, biopsies were dispersed in 750 µL of phosphate buffer (pH 5.4) and, with an Ultra-Turrax T25 homogenizer (IKA1 Werke GmbH & Co. KG, Staufen, Germany), were homogenized in a ice bath. The supernatant obtained after centrifugation was diluted with PBS 5.4 (1:10) in order to assay MPO activity. Briefly, in a 96-well plate, 10 µL of diluted sample, 20 µL of sodium phosphate buffer (pH 5.4), 200 µL of phosphate buffer (pH 7.4), 40 µL of 0.052% hydrogen peroxide and 20 µL of 18 mM 3,30,5,50-tetramethylbenzidine dihydrochloride were added to each well. At the end of experiment, 50 µL of SO_4H_2 2N was added to stop the reaction. The absorbance was measured at 450 nm. The MPO activity was calculated from the linear portion of a standard curve.

2.9. Histological examination

Mice skin was excised, fixed and stored in formaldehyde (0.4%, V/V). Longitudinal sections (5 mm) were marked with hematoxylin and eosin and observed using a light microscope (DMD 108 Digital Micro-Imaging Device, Leica, Wetzlar, Germany).

2.10. Statistical analysis of data

Statistical differences were determined by one-way ANOVA test and Tukey's test for multiple comparisons with a significance level of $p < 0.05$. All statistical analyses were performed using

ACCEPTED MANUSCRIPT

IBM SPSS statistics 22 for Windows (Valencia, Spain). Data are shown as mean ± standard deviation.

3. Results and discussions

3.1. Analytical method

The analytical method (HPLC) for NA quantification was firstly validated. Calibration curves covering the whole range of NA concentrations were prepared. Excellent plots correlating the peak areas and NA concentrations were obtained ($r > 0.999$), demonstrating good linearity. Precision was evaluated by calculating the relative error (RE, %) and accuracy by coefficient of variation (CV, %); both values were less than 9 %. The limits of detection (LOD) and quantification (LOQ) were 0.11 µg/mL and 0.34 µg/mL, respectively. These data satisfy the standard validation.

3.2. Physicochemical properties

The flavanone glycoside (NA) was characterized with the RX technique. The spectrum shows that it is a flavonoid with crystalline structure. Molecules are spatially distributed in a regular and symmetrical form, so they require more energy for their separation. All this property may be responsible of their low solubility and bioavailability. Indeed, the solubility of NA in water and phosphate buffer at pH 7.4 is 2.69±0.01 mg/mL and 1.94 ± 0.01 mg/mL, respectively. As it was expected, NA is more soluble (14.4±0.4 mg/mL) in presence of polysorbate 80 (1%, w/w), probably because of the formation of micelles, which allows the solubilization of a greater amount of flavonoid. In addition, NA is a hydrophilic compound ($\log P_{oct} = -0.66 \pm 0.03$) with a molecular weight superior to 580 g/mol, which could lead to a low percutaneous absorption.

3.3. Characterization of Ultradeformable liposomes

In Figure 2 the formation of spherical nanometric vesicles can be observed. All ultradeformable liposomes (I, II and III) showed a monodisperse distribution (PI < 0.30) (Table 1). In all cases, the mean size was very similar (approximately 100 nm), and no statistical differences were

ACCEPTED MANUSCRIPT

observed from batch to batch. The zeta potential was highly negative (-30 mV), for the different NA concentrations. Liposomes were able to incorporate NA in high amount (entrapment efficiency approximately 90%), no significant differences were detected among the groups ($p > 0.05$), confirming that the flavonoid was effectively/efficiently incorporated into vesicle. Ultradeformable liposomes were stable during 30 days of storage, according to zeta potential and mean size values (Table 1). Such data ensure good stability of ultradeformable liposomes, due to the great electrostatic repulsion between the vesicles.

3.4. Cell viability studies

The biocompatibility of each formulation was evaluated *in vitro* on cells, which represents a good and reliable method to select formulations that will be used for further *in vivo* studies. 3T3 mouse dermal fibroblasts were incubated with different formulations: empty or NA ultradeformable liposomes (I, II and III). Cells viability after 24 hours of incubation with the formulation is approximately 100% and similar to that of the control group ($p > 0.05$). These results are in accordance with Cao et al [34], confirming the low toxicity of flavonoid and liposomes.

3.5. *In vitro* diffusion

Permeation study was performed for 24 h using ultradeformable liposomes (I, II and III). Figure 3 shows the cumulative amounts (Q, %) of NA in the donor compartment (CD), epidermis (EP) and receptor compartment (CR) for all formulations tested at 24 hours. The cumulative amount of NA (%) in the CR was negligible (less than 0.5 %) regardless the formulation tested. The amounts (%) of NA accumulated in the EP (~ 10%) could explain the anti-inflammatory properties of ultradeformable liposomes detected during the *in vivo* assay. Finally, the amount of NA present in the CD (> 90 %), confirmed the low flavonoid bioavailability. The NA low permeability could be mainly attributed to its difficulty to permeate through the stratum corneum, which serves as a lipophilic barrier against the penetration of hydrophilic molecules (NA has log

ACCEPTED MANUSCRIPT

P oct = - 0.66). In addition, the high molecular weight (~580 g/mol) of NA could have limited its transdermal delivery by the high resistance of skin towards diffusion [35, 36].

3.6. *In vivo* assay

TPA application in mice has been used for the evaluation of anti-inflammatory activity of drugs. This compound induces a variety of histological and biochemical changes in the skin [37]. In this work, TPA was daily applied on mice dorsal skin for 3 days, inducing skin ulceration, loss of epidermis integrity with scale and crust formation. Besides, it stimulates the oedema formation, due to an increase in vascular permeability. Table 2 summarizes the results obtained. The phorbol ester (TPA) caused a 3-fold increase in skin weight, compared to healthy mice. The administration of liposomes I, II and III was more active than NA dispersion and betamethasone cream in reducing skin oedema (~20%). Statistical differences were observed between samples ($p < 0.01$), probably because the ultradeformable liposomes promoted the internalization of NA in epithelial cells, avoiding vascular congestion and oedema formation. The MPO activity was quantified as a marker of the inflammatory process, since it is proportional to the neutrophil concentration in the inflamed tissue. The efficacy of NA loaded ultradeformable liposomes was assayed and compared with betamethasone cream, as commercial reference, and NA dispersion. The ultradeformable liposomes displayed a superior ability to reduce MPO activity in the injured tissue respect to the betamethasone cream (Table 2). No significant differences were observed ($p > 0.05$) between the three vesicular formulations containing different amounts of NA, which indicates that, in our experimental conditions, ultradeformable liposomes can promote the NA beneficial activity independent of the concentration used. Liposomes (III) have a greater activity respect to NA dispersion ($p < 0.01$), despite having the same concentration of flavonoid, as shown in Table 2. Thus, this phospholipidic system could be considered as promising tools for treatment of skin inflammation. The macroscopic observations are in agreement with the MPO and oedema values.

ACCEPTED MANUSCRIPT

The macroscopic images of mice clearly showed the positive effect of NA ultradeformable liposomes on injured skin (Figure 4).

With regard to the histological study, morphological alterations of mice skin exposed to TPA were evaluated by hematoxylin and eosin staining, and compared with untreated skin (Figure 5). The skin treated with acetone only (control -) showed a regular structure and normal appearance of both epidermis and dermis, as well as the tissues directly underneath (i.e., subcutaneous cellular tissue, skeletal muscle and adipose tissue), with only some mononuclear and polymorphonuclear cells in the muscular region. Otherwise, mice skin treated with TPA displayed severe dermal and subcutaneous alteration, with a large number of leukocytes infiltrating, and showing pathological features of inflammatory damage, such as vascular congestion (control +). Similar results of injured skin were obtained using betamethasone cream, but the application of the NA ultradeformable liposomes reduced TPA-induced lesions, along with mild to moderate inflammatory infiltrates of mononuclear cells, eosinophils and neutrophils. Therefore, the results obtained *in vivo* seem to indicate a remarkable therapeutic potential of NA ultradeformable liposomes.

4. Conclusions

The loading of NA into ultradeformable liposomes represents an innovative approach to prevent and treat skin lesion and restore skin integrity. Results demonstrated that NA liposomes were highly biocompatible and more effective than betamethasone cream and NA dispersion as demonstrate *in vivo* model (TPA test). In conclusion NA ultradeformable liposomes can be considered as a promising formulation for the treatment of inflammatory diseases.

Ackwonledgment

We wish to express our gratitude to Lipoid GmbH (Ludwigshafen, Germany) for providing the phospholipid used in this work for free.

References

ACCEPTED MANUSCRIPT

[1] Chen H, Lu C, Liu H, Wang M, Zhao H, Yan Y et al, 2017. Quercetin ameliorates imiquimod-induced psoriasis-like skin inflammation in mice via the NF-κB pathway. International Immunopharmacology. 48, 110-117.

[2] Parmar KM, Itankar PR, Joshi A, Prasad SK, 2017.Anti-psoriatic potential of Solanum xanthocarpum stem in Imiquimod-induced psoriatic mice model.Journal of etnopharmacology.23(198),158-166.

[3] Manca M. L., Castangia I, Zaru M, Nácher A, Valenti D, Fernàndez-Busquets et al, 2015. Development of curcumin loaded sodium hyaluronate immobilized vesicles (hyalurosomes) and their potential on skin inflammation and wound restoring. Biomaterials. 71, 100-109.

[4] Caddeo C, Nacher A, Vassallo A, Armentano M. F., Pons R, Fernàndez-Busquets et al,2016. Effect of quercetin and resveratrol co-incorporated in liposomes against inflammatory/oxidative response associated with skin cancer. International journal of pharmaceutics. 513(1), 153-163.

[5] Castro-Vazquez L, Alañon M, Rodriguez-Robledo V, Pérez-Coello M S, Hermosín-Gutierrez, Díaz-Maroto M C, 2016. Bioactive Flavonoids, Antioxidant Behaviour, and Cytoprotective Effects of Dried Grapefruit Peels (Citrus paradisi Macf.). Oxidative Medicine and Cellular Longevity. 2016, 2016:8915729.

[6] Manconi M, Manca M. L, Marongiu F, Caddeo C, Castangia I, Petretto et al, 2016. Chemical characterization of Citrus limon var. pompia and incorporation in phospholipid vesicles for skin delivery. International journal of pharmaceutics.506 (1), 449-457.

[7] Chen R, Qi Q L, Wang M T, Li Q Y, 2016. Therapeutic potential of naringin: an overview. Pharmaceutical Biology.54 (12), 3203-3210.

[8] Ramakrishnan A, Vijayakumar N, Renuka M, 2016. Naringin regulates glutamate-nitric oxide cGMP pathway in ammonium chloride induced neurotoxicity. Biomedecine and pharmacotherapie.84:1717-1726.

ACCEPTED MANUSCRIPT

[9] Ahmad S. F, Attia S. M, Bakheet S. A, Zoheir K. M, Ansari M. A, Korashy H. M, et al, 2015. Naringin attenuates the development of carrageenan-induced acute lung inflammation through inhibition of NF-κb, STAT3 and pro-inflammatory mediators and enhancement of IκBα and anti-inflammatory cytokines. Inflammation.38 (2), 846-857.

[10] Gopinath K, Sudhandiran G, 2012. Naringin modulates oxidative stress and inflammation in 3-nitropropionic acid-induced neurodegeneration through the activation of nuclear factor-erythroid 2-related factor-2 signalling pathway. Neuroscience. 227, 134-143.

[11] Luo Y. L, Zhang C. C, Li P. B, Nie Y. C, Wu H, Shen J. G. et al, 2012. Naringin attenuates enhanced cough, airway hyperresponsiveness and airway inflammation in a guinea pig model of chronic bronchitis induced by cigarette smoke. International immunopharmacology.13 (3), 301-307.

[12] Guihua X, Shuyin L, Jinliang G, Wang S, 2016. Naringin protects ovalbumin-induced airway inflammation in a mouse model of asthma. Inflammation. 39(2), 891-899.

[13] Itoh K., Masuda M., Naruto S., Murata K., Matsuda H ,2009. Antiallergic activity of unripe Citrus hassaku fruits extract and its flavanone glycosides on chemical substance-induced dermatitis in mice. Journal of natural medicines.63 (4), 443-450.

[14] Tamer A. ElBayoumi and Vladimir P. Torchilin. 2010. Current trends in liposomes research in Liposomes Methods and Protocols, Volkmar Weissig (eds.) volume 1, cap. 1, pp.1-27.

[15] S.Vahabi ,A.Eatemadi,2017.Nanoliposomes encapsulated anesthetics for local anesthesia application. Biomedicine Phaemacotherapy.86,1-7.

[16] N.Kianvash, A.Bahador, M Pourhajibagher, H Ghafari, V Nikoui ,SM Rezayat. et al, 2017.Evaluation of propylene glicol nanoliposomes containing curcumin on burn wound model in rat:biocompatibility, wound healing, and anti-bacterial effects. Drug Delivery and Translational Research.

ACCEPTED MANUSCRIPT

[17] J Rokka, A Snellman, M Kaasalainen, J Salonen, C Zona, B La Ferla et al,2016. (18) F-labeling syntheses and preclinical evaluation of functionalized nanoliposomes for Alzheimer`s disease. European Journal of Pharmaceutical Sciences.10 (88),257-266.

[18] P Ganesan, HM Ko, IS Kim, DK Choi, 2015.Recent trends in the development of nanophytobioactive compounds and delivery systems for their posible role in reducing oxidative stress in Parkinson`s disease models.International Journal Nanomedicine.10,6757-6772.

[19] MM Ochi, G Amoabediny, SM Rezayat, A Akbarzadeh, B Ebrahimi, 2016.In vitro Co-Delivery of Novel Pegylated Nanoliposomal Herbal Drugs of Silibinin and Glycyrrhizic Acid (Nano-Phytosome) to Hepatocellular Carcinoma Cells.Cell.18(2),135-148.

[20] HJ Park, N Liu, 2010.Factors effects on the loading efficiency of Vitamin C loaded chitosan-coated nanoliposomes. Colloids and Surfaces B: Biointerfaces.76 (1),16-19.

[21] S Yang, C Liu, W Liu, H Yu, H Zheng, W Zhou et al, 2013.Preparation and characterization of nanoliposomes entrapping medium-chain fatty acids and vitamin C by lyophilization. International Journal of Molecular Sciences.14(10),19763-19773.

[22] M.R. Mozafari, 2010.Nanoliposomes: Preparation and Analysis in Liposomes Methods and Protocols, Volkmar Weissig (eds.) volume 1, cap. 2, pp.29-50.

[23] Kakadia PG, Conway BR, 2015.Lipid nanoparticles for dermal drug delivery. Current pharmaceutical design. 21(20), 2823-2829.

[24] Mir-Palomo S, Nácher A, Díez-Sales O, Ofelia Vila Busó MA, Caddeo C, Manca ML et al, 2016. Inhibition of skin inflammation by baicalin ultradeformable vesicles. International Journal of Pharmaceutics. 511(1):23-29.

[25] Vitonyte J, Manca M. L., Caddeo C, Valenti D, Peris J. E., Usach I et al, 2017. Bifunctional viscous nanovesicles co-loaded with resveratrol and gallic acid for skin protection against

ACCEPTED MANUSCRIPT

microbial and oxidative injuries. European Journal of Pharmaceutics and Biopharmaceutics. 114, 278-287.

[26] Kianvash N, Bahador A, Pourhajibagher M, Ghafari H, Nikoui V, Rezayat S. M. et al,2017. Evaluation of propylene glycol nanoliposomes containing curcumin on burn wound model in rat: biocompatibility, wound healing, and anti-bacterial effects. Drug Delivery and Translational Research.1-10.

[27] Chen J, Lu W. L, Gu W, Lu S. S, Chen Z. P, Cai B. C ,2013. Skin permeation behavior of elastic liposomes: role of formulation ingredients. Expert opinion on drug delivery.10 (6), 845-856.

[28] Cordenonsi LM, Bromberger NG, Raffin RP, Scherman EE, 2016.Simultaneous separation and sensitive detection of naringin and naringenin in nanoparticles by chromatographic method indicating stability and photodegradation kinetics. Biomedical chromatography. 30(2), 155-162.

[29] Morikawa G, Suzuka C, Shoji A, Shibusawa Y, Yanagida A,2016. High-throughput determination of octanol/water partition coefficients using a shake-flask method and novel two-phase solvent system. Journal of Pharmaceutical and Biomedical Analysis. 117,338-344.

[30] Harris WM, Zhang P, Plastini M, Ortiz T, Kappy N, Benites J, et al, 2017.Evaluation of function and recovery of adipose-derived stem cells after exposure to paclitaxel. Cytotherapy.19 (2), 211-221.

[31] Chilcott RP, Jenner J, Hotchkiss S. A. M, Rice P, 2001. In vitro skin absorption and decontamination of sulphur mustard: comparison of human and pig-ear skin. Journal of applied toxicology. 21(4), 279-283.

[32] Merino V., Micó- Albiñana T., Nácher A., Díez- Sales O., Herráez M.,Merino- Sanjuán, M. 2008. Enhancement of nortriptyline penetration through human epidermis: influence of chemical enhancers and iontophoresis. Journal of Pharmacy and Pharmacology, 60(4), 415-420.

ACCEPTED MANUSCRIPT

[33] Sato H, Nakayama Y, Yamashita C, Uno H, 2004. Anti-inflammatory effects of tacalcitol (1, 24(R) (OH) 2D3, TV-02) in the skin of TPA-treated hairless mice. The Journal of Dermatology.31 (3), 200-217.

[34] Cao X, Lin W, Liang C, Zhang D, Yang F, Zhang Y, et al,2015. Naringin rescued the TNF-α-induced inhibition of osteogenesis of bone marrow-derived mesenchymal stem cells by depressing the activation of NF-κB signaling pathway. Immunologic Research.62 (3):357-367.

[35] Han T., Das, D. B., 2013. Permeability Enhancement for Transdermal Delivery of Large Molecule Using Low- Frequency Sonophoresis Combined with Microneedles. Journal of pharmaceutical sciences.102 (10), 3614-3622.

[36] Gao Y., Ni J., Yin X., Shen, X, 2010. Study on transdermal absorption of piperine in Erxiekang plaster. Journal of Chinese materia médicaper. 35(24), 3294-3296.

[37] Caddeo C, Sales O.D, Valenti D, Saurí A.R, Fadda A.M, Manconi M, 2013. Inhibition of skin inflammation in mice by diclofenac in vesicular carriers: liposomes, ethosomes and PEVs. International journal of pharmaceutics. 443(1), 128–136.

Figures

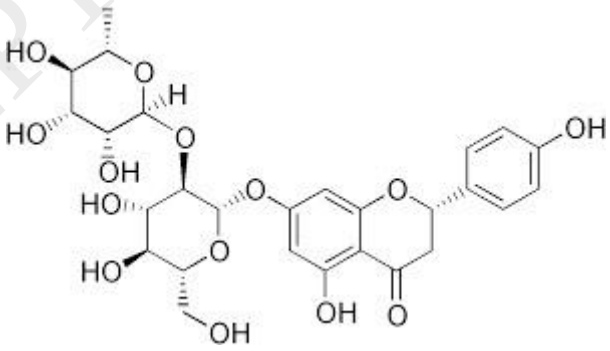

Figure 1. Chemical structure of Naringin (NA).

ACCEPTED MANUSCRIPT

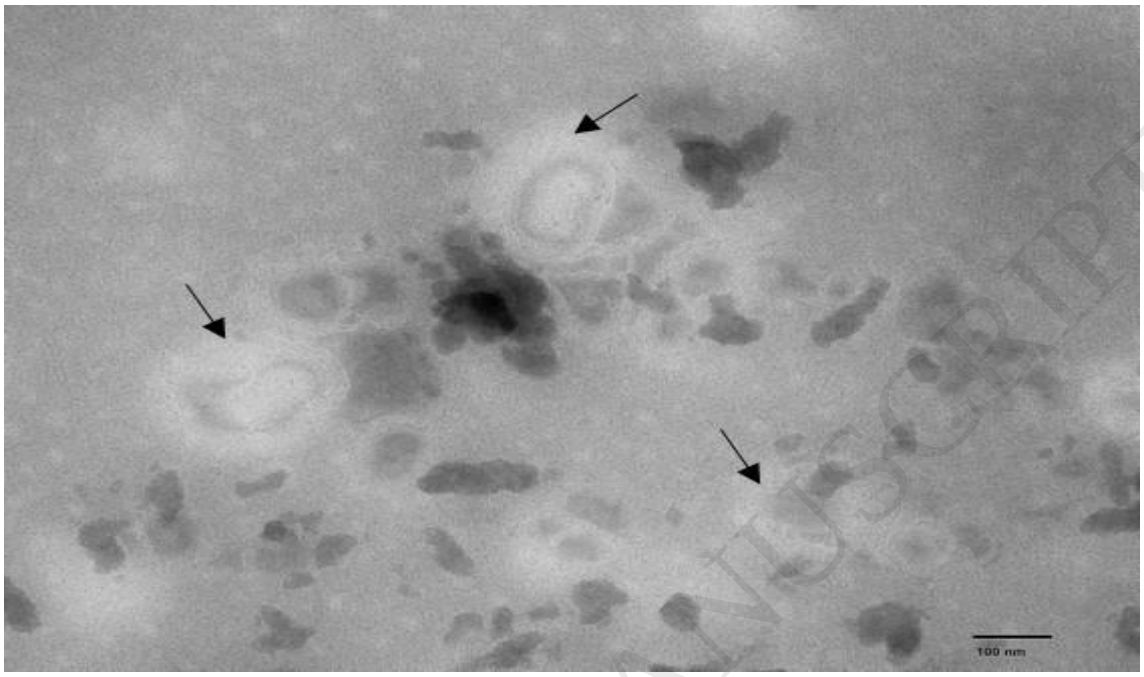

Figure 2. TEM (Transmission electron microscopy) images of ultradeformable liposomes. The arrows indicate the lamellae of vesicles.

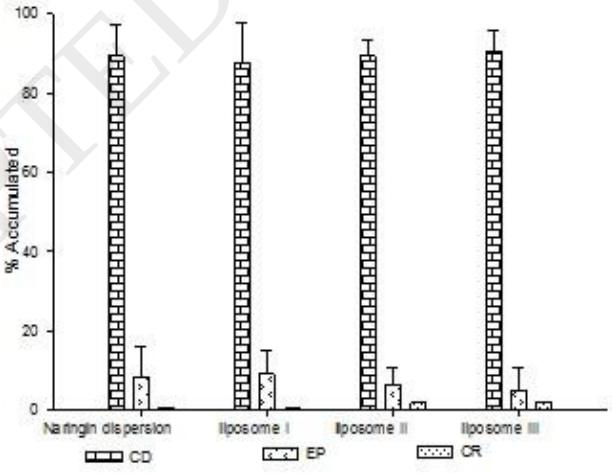

Figure 3. Transdermal permeation of NA (naringin) dispersion and loading liposomes I (3 mg/mL), II (6 mg/mL), III (9 mg/mL). Amount accumulated in CR (receptor compartment), CD (donor compartment) and EP (epidermis) after

ACCEPTED MANUSCRIPT

24 h at 32°C. The results were expressed as the mean and standard deviation (error bars). No significate differences have been found among the groups ($p > 0.05$).

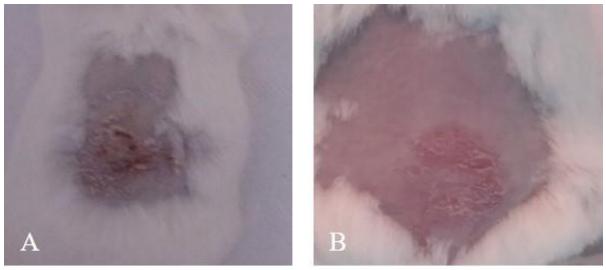

Figure 4. Macroscopic appearance of mice skin lesions inducted with TPA (A) and treated with liposome III: 9 mg/mL (B).

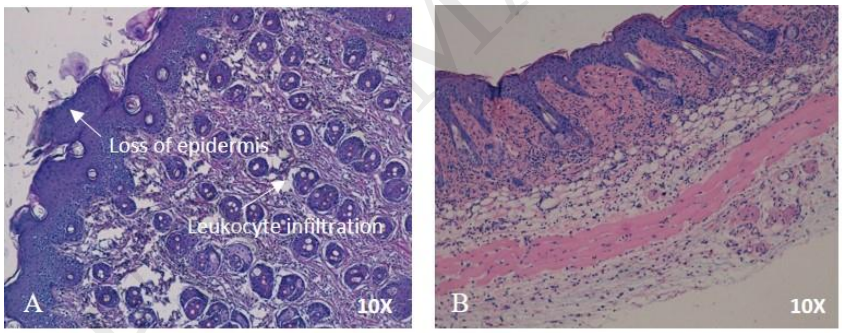

Figure 5. Representative histological sections of mouse skin: treated with TPA-inflamed skin (A) and treated with liposome III: 9 mg/mL (B).

Tables

ACCEPTED MANUSCRIPT

Formulations	Size (nm)			PI			Potential Z (mV)		EE (%)
	0 days	30 days		0 days	30 days		0 days	30 days	
Empty liposome	88.3 ± 1.7	100.1 ± 0.8		0.25	0.16		-32.5 ± 0.4	-31.9 ± 1.7	---
Liposome I	90.2 ± 1.6	90.9 ± 2.3		0.23	0.22		-33.9 ± 1.4	-30.1 ± 1.1	91.03 ± 0.04
Liposome II	86 ± 1.0	84.1 ± 2.5		0.25	0.20		-32.6 ± 1.1	-26.9 ± 0.8	88.70 ± 0.25
Liposome III	86.3 ± 1.1	84.6 ±0.9		0.22	0.22		-27.7 ± 1.1	-28.0 ± 1.5	92.72 ± 0.10

Table 1. Average size, polydispersity index (PI), zeta potential and NA (naringin) entrapment efficiency of liposome I (3 mg/mL), liposome II (6 mg/mL) and liposome III (9 mg/mL). All values are mean ± standard deviations (n=3).

Formulations	% Oedema inhibition		% MPO inhibition
Control +	0.5 ± 1.15		0.5 ±1.01
Cream	13.06 ± 2.81		12.70 ± 1.81
NA dispersion	27.48 ± 3.37		65.82 ± 2.94
Empty liposome	23.67 ± 2.29		60.25 ± 3.05
Liposome I	36.01* ± 3.03		74.61 ± 4.03
Liposome II	37.29* ± 3.19		78.72 ± 4.59
Liposome III	43.18* ± 3.36		86.75# ± 4.93

Table 2. Oedema inhibition and MPO (myeloperoxidase test) activity in skin mice inflamed with TPA (control +). Skin mice inflamed were treated to 200 µL of NA dispersion, empty liposomes or loading liposomes I (3 mg/mL), II (6 mg/mL), III (9 mg/mL) and betamethasone cream (20 mg). The results were expressed as the mean and standard deviation (error bars). * $p < 0.01$ liposomes (I, II and III) vs betamethasone cream and NA dispersion. ANOVA-Tukey. # $p < 0.01$ liposome III vs NA dispersion. ANOVA-Tukey.